

Effect of Noise on Vibrational Resonance at the Beat Frequency in a Bistable Vertical-Cavity Surface-Emitting Laser with a Biharmonic Excitation

V. N. Chizhevsky*

B.I. Stepanov Institute of Physics, National Academy of Sciences of Belarus, 220072 Minsk, BELARUS

Nianqiang Li

*School of Optoelectronic Science and Engineering,
Soochow University, Suzhou 215006, CHINA*

(Received 10 September, 2023)

The results of an experimental and theoretical study of the effect of noise on the polarization dynamics of a bistable vertical-cavity surface-emitting laser (VCSEL) driven by two harmonic signals with the frequencies f_1 and $f_2 = 2f_1 + \delta$, where $\delta < f_1$ is the detuning frequency, is presented. In the noiseless case, the response amplitude at the beat frequency δ is higher than the response in conventional vibrational resonance (VR) at the frequency f_1 . In the presence of noise, the method of the detection on the beat frequency can be more effective in a certain range of noise intensity as compared to the traditional VR method. The experimental results are in good agreement with the numerical results obtained within the framework of the model of a bistable overdamped oscillator.

PACS numbers: 5.45.-a, 42.55.Px, 42.65.Sf, 42.60.Mi

Keywords: surface-emitting laser, noise, bistable overdamped oscillator

DOI: <https://doi.org/10.5281/zenodo.10034467>

1. Introduction

Bistable systems can be used as detectors of weak subthreshold low-frequency (LF) or cv signals through the phenomenon of stochastic resonance [1] or vibrational resonance (VR) [2]. In the latter case the response of a bistable system to the effect of the subthreshold periodic excitation can be greatly enhanced by an additional high-frequency (HF) periodic force. The phenomenon of VR shows up as the resonance-like behavior depending on the amplitude or the frequency of the superimposed HF signal. The mechanism underlying VR is an amplification near the critical point corresponding to transition from bistability to monostability controlled by the HF signal [3, 4]. The phenomenon of VR was demonstrated and studied experimentally in analog electric

circuits [5–9], a bistable vertical-cavity surface-emitting laser (VCSEL) [10–15], optic lattice [16], mechanical systems [17], a driven nano resonator [18], optomechanical nanocavity [19]. Theoretical investigations have revealed phenomenon of VR in various nonlinear systems from different fields such as, for instance, neural systems [20–23], coupled oscillators [24–27], multistable systems with the periodic potential [28], delayed multistable systems [29], fractional-order systems [30], and nonlinear maps [31–33]. Some examples of the occurrence of vibrational resonance in diverse dynamical systems can be found also in the book by Rajasekar and Sanjuán [34] and in papers [35, 36]. Most of the investigations were performed for the resonant case when the frequency of the HF signal is a multiple number (k) of the frequency of the input signal and much larger in magnitude ($k \gg 1$). In this case the phase difference between two periodic signals has only an insignificant effect on the response

*E-mail: vnc@dragon.bas-net.by

of bistable system at the frequency of the LF signal. Frequency-resonance-enhanced vibrational resonance was studied by Yao *et al* [37] where it was found that the maximal response occurs when both frequencies coincide ($k=1$) with zero phase difference between two harmonic signals.

The generation of higher harmonics or combinational frequencies is a characteristic feature of driven dynamical systems with a nonlinear transfer function and it can be observed in different fields. In this context, ghost-vibrational resonance at a fundamental frequency missing in the multifrequency input signal induced by a high-frequency signal in bistable systems was demonstrated [38–40]. It was shown experimentally that VR in a bistable VCSEL with a biharmonic excitation is accompanied by the appearance of higher-order harmonics of the LF signal [41]. Theoretical investigations of a resonant behavior on subharmonic and superharmonic frequencies which are not an integer multiple of the low frequency in vibrational resonance were performed in [42].

The effect of noise on VR was also studied in different systems both theoretically [6, 11, 12, 43–46] and experimentally [8, 11–13]. These papers were devoted to study the effect of noise on the first harmonic of the LF response of nonlinear systems. It was shown in these investigations that the addition of noise lead to decreasing the LF response amplitude, broadening the LF response curve and the shift of the optimal value of the HF amplitude as the noise strength increases. In particular, scaling laws for the gain factor, the signal-to-noise ratio and the shift of the optimal HF amplitude depending of the added noise intensity were found experimentally in a VCSEL [11, 12]. It is important that the use of vibrational resonance allows one to obtain higher signal-to-noise ratio than stochastic resonance does [12, 47].

This paper presents the results of an experimental and theoretical study of the effect of noise on the response of a bistable vertical cavity surface emitting laser (VCSEL) at the beat frequency when excited by two harmonic signals with frequencies f_1 and $f_2 = 2f_1 + \delta$,

where δ is a detuning frequency, and noise with a normal distribution and zero average. Such a type of the detection approach can be considered as vibrational resonance on the beat frequency. In this work, the main attention is paid to comparing the robustness of detection of weak subthreshold signals to the effect of noise at the beat frequency δ with a conventional detection at the frequency of the signal under study f_1 , i.e. within the framework of VR.

2. Experimental and methods

Investigations were performed on the experimental setup similar to earlier used for studying the resonant behaviour of higher-order harmonics in VR [41, 48]. A 850-nm VCSEL (Honeywell HFE4080-321) with a threshold current $J_{th} \approx 5.6$ was used. The temperature of the laser diode was controlled to an accuracy of 0.01°C . The measurements were performed at temperature of the laser diode set to 17.5°C . A half-wave plate and a Glan's prism were used in order to split the collimated laser emission into two polarization components.

The temporal laser responses on one selected polarization were recorded by a fast photodiode and USB-oscilloscope. Two harmonic signals from function generators with frequencies $f_1 = 1$ kHz and $f_2 = 2f_1 + \delta$ were added to the dc current. The case of commensurate input frequencies f_1 and δ was studied here. The amplitudes of both periodic signals were changed over a wide range of values. Two cases were studied here. In the first case, the amplitude A_2 is a control parameter whereas the input subthreshold signal is at the frequency f_1 . In the second case, the input signal is at the frequency f_2 while the control signal at the frequency f_1 . All investigations were performed in the adiabatic regime of excitation when both signal frequencies are less than the cutoff frequency of the amplitude-frequency characteristic of the polarization-resolved laser response. The Gaussian white noise from an arbitrary waveform generator with a bandwidth of

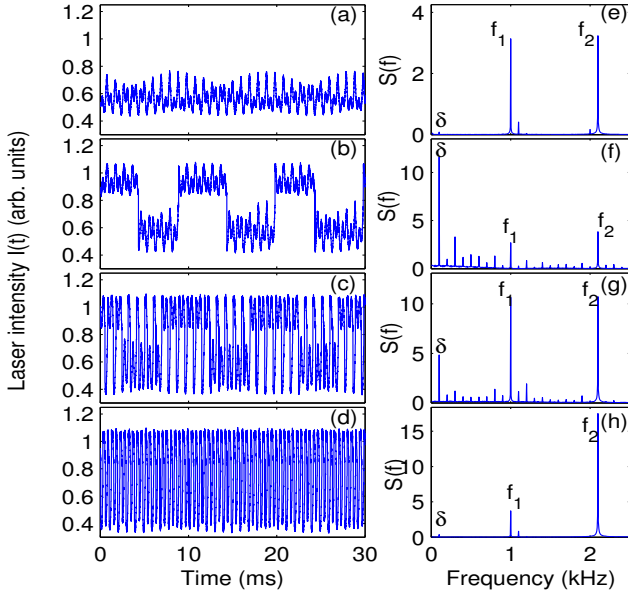


FIG. 1. Experiment. Left panel: Temporal behavior of the laser intensity for different values of the amplitude A_2 , $A_2 = 46$ (a), 56.8 (b), 103 (c), 137 (d) mV. Right panel: Amplitude spectra $S(f)$ of the temporal laser responses shown for the same values of A_2 as in the left panel; $A_1=35$ mV, $f_1=1$ kHz, $f_2=2.1$ kHz.

2 MHz with different amplitude σ_N (rms) was also added to the dc current. In what follows, the noise strength is defined as $D_{exp} = \sigma_N^2$. The parameters controlled from computer during the experiments were the noise intensity σ_N^2 , the frequencies f_1 and f_2 , and the signal amplitudes A_1 and A_2 .

The numerical simulation was carried out in the framework of a Langevin equation with a double-well potential which widely used in studying nonlinear phenomena in bistable systems in different fields. It was shown that this model excellently agrees with the experimental observation of higher-order harmonics and noise-induced suppression of nonlinear distortions in vibrational resonance in a bistable VCSEL [41, 48]. In this case the equation reads

$$\frac{\partial x}{\partial t} = -V'(x) + A_1 \sin(2\pi f_1 t) + A_2 \sin(2\pi f_2 t) + \zeta(t), \quad (2.1)$$

where $V'(x)$ is the derivative with respect to x of a bistable potential function $V(x)$, f_1 and $f_2 =$

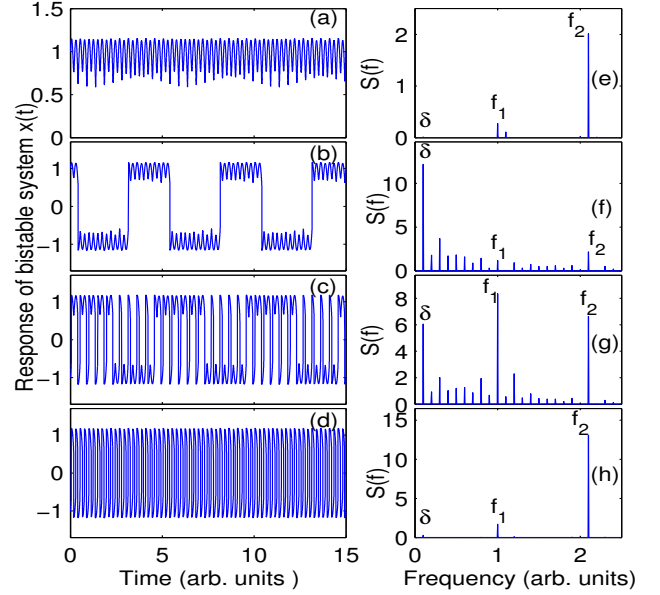


FIG. 2. Simulation. Left panel: Temporal responses of the bistable system (see Eq. (2.1)) for different values of the control amplitude A_2 , $A_2 = 1.39$ (a), 1.42 (b), 1.5 (c), 1.7 (d). Right panel: Amplitude spectra $S(f)$ of the temporal responses shown for the same values of A_2 as in the left panel.

$2f_1 + \delta$ are excitation frequencies, δ is a detuning frequency and $\zeta(t)$ is a white, Gaussian noise with $\langle \zeta(t)\zeta(t') \rangle = 2D\delta(t-t')$ and mean $\langle \zeta(t) \rangle = 0$. A bistable potential function $V(x)$ in the following form was used: $V(x) = x^4 - 2x^2$. Throughout the simulation $f_1=0.001$ and $f_2=0.0021$ were used. Similar to the experiment the frequencies f_1 and f_2 are commensurate quantities with the same ratios f_1/δ as also are in the experiment. The simulation was performed in the adiabatic regime when both periodic forces were very slow with respect to the intrawell relaxation times. In what follows, the experimental results and the corresponding numerical ones will be described together.

3. Results

First, the temporal polarization dynamics in a VCSEL was investigated for a fixed value of the amplitude A_1 depending on amplitude

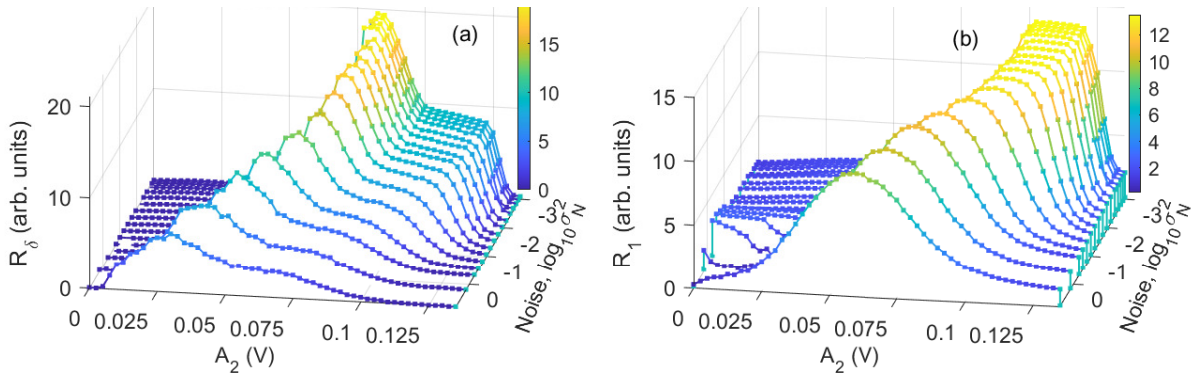


FIG. 3. Experiment. Response of a bistable VCSEL at the frequencies (a) δ and (b) f_1 for different values of added noise intensity σ_N^2 . Control signal is at the frequency f_2 . $A_1 = 0.025$ V, $f_1 = 1$ kHz, $f_2 = 2.1$ kHz.

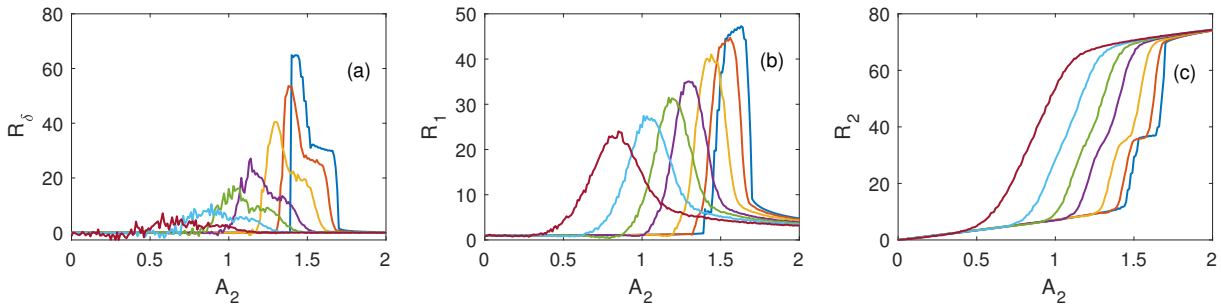


FIG. 4. Simulation. Response of a bistable system at frequencies (a) δ , (b) f_1 and (c) f_2 for different values of added noise, D . The control signal is at the frequency f_2 . $A_1 = 0.15$, $f_1 = 0.001$, $f_2 = 0.0021$.

A_2 of the control signal for the case of the symmetrical configuration of the bistable potential. Some temporal laser responses on the selected polarization are shown in the left panel in Fig. 1. The right panel in Fig. 1 shows the corresponding spectra.

For the amplitude $A_2 = 46$ mV (see Fig. 1(a)) near the switching threshold one can see in the temporal behavior oscillations with a weak slowly varying amplitude on the frequency δ where dominant frequencies are f_1 and f_2 (see Fig. 1(e)). An increase of the amplitude A_2 up to 56.8 mV leads to an appearance of clear-cut switchings between polarization states at the frequency δ (Fig. 1(b)) and, correspondingly, gives rise to the high response amplitude R_δ at the frequency δ in the spectrum of the signal which is well above the response amplitudes R_1 and R_2 at the frequencies f_1 and f_2 , respectively

(see Fig. 1(f)). A further increase of A_2 results in the appearance of the switchings at the frequency f_1 in the temporal behavior of laser intensity (see Fig. 1(c)) and, respectively, the increase of the response amplitude R_1 (see Fig. 1(g)). For the values of A_2 above 128.8 mV the temporal behavior is determined mainly by the control signal (see Fig. 1(d)) with dominant frequency f_2 (see Fig. 1(h)). A very similar temporal behavior is observed in the numerical simulation shown in Fig. 2.

Figure 3 shows the results of the experimental study of the effect of noise on the response of a bistable VCSEL at the beat frequencies δ (Fig. 3(a)) and the input signal frequency f_1 (Fig. 3(b)). The response amplitudes R_δ , R_1 and R_2 in the experimental and numerical studies were estimated as the height of the peaks in the spectra of the time series at the frequencies

δ , f_1 and f_2 , respectively.

From the data presented in the Fig. 3, one can see that the effect of noise leads to a decrease of the response amplitudes for both spectral components δ and f_1 , a broadening of their response curves depending on the amplitude of the control signal A_2 and shift of the optimal value of the amplitude of the control signal A_2 towards lower values. Similar peculiarities are observed in the numerical simulation which results are presented in Fig. 4. One can note that noise results also in the smoothing of the response at the frequency of the control signal (see Fig.4(c)).

A quantitative comparison of the effect of noise on these spectral components is shown in Fig. 5 for both experimental (see Figs. 5(a) and 5(b)) and numerical (see Figs. 5(c) and 5(d)) results. The plots show the maximal values of the responses (R_δ^{max} and R_1^{max}) versus the magnitude of the added noise intensities σ_N^2 (D in the simulation) normalized to the response amplitude R_δ at zero noise intensity and the optimal values of the control amplitude A_2 for both spectral components. It can be seen that in a certain range of noise intensity $R_\delta^{max} > R_1^{max}$, which can be used for more efficient detection of subthreshold signals in bistable systems. At the same time one can note that the optimal values of the amplitude of the control signal ($A_{2,\delta}^{opt}$ and $A_{2,1}^{opt}$), corresponding to the maximum values of the responses, differ slightly, thus, that $A_{2,\delta}^{opt} < A_{2,1}^{opt}$ for the whole noise range used in the experiments and the numerical simulation. One can note a rather good qualitative agreement between experimental and numerical results.

Similar studies were carried out for the case when the input signal was at the frequency f_2 , and the control signal was at the frequency f_1 . These results are shown in the figure 6. It can be seen that, in contrast to the previous case, for $\sigma_N^2 = 0$ the response at the beat frequency is much greater than the response at the frequency of the input signal. In this case, the addition of noise has a different effect on the spectral components. In particular, an increase in the intensity of the added noise leads to a decrease in the maximum

amplitude, a broadening of the response curve, and a shift in the optimal value of the response at the beat frequency (Figs. 6(a) and 6(d)). At the same time, the maximum value of the response at the frequency of the input signal almost does not depend on the intensity of the added noise (Fig. 6(b) and 6(e)). For the whole range of the noise intensity, the maximum values $R_\delta^{max} > R_2^{max}$. This can be clearly seen in Fig. 7, which shows the experimental (Fig. 7(a)) and numerical (Fig. 7(b)) values of R_δ^{max} and R_2^{max} as a function of noise intensity. One can note again a good agreement of experimental and numerical results presented in the Figs. 6 and 7.

4. Conclusion

To summarize, we have presented the experimental and numerical results which demonstrate that the response on the beat frequency in a bistable system driven by two harmonic signals with a small difference from their multiple ratio can be large enough to be comparable with the response in vibrational resonance. What is more, the advantage of the detection on the beat frequency is a decrease of the frequency of the additional control modulation with elimination of the necessity for phase synchronization signals using close frequencies in the resonant case. Such an approach, therefore, can be useful from the practical standpoint as a method of the detection of weak periodic signals, or the method of an effective generation of the well-controllable low-frequency signals. A study of the influence of noise on the response of a bistable system shows that in a certain range of noise intensity the detection at the beat frequency can be quite effective and a more preferable as compared to the traditional vibration resonance approach.

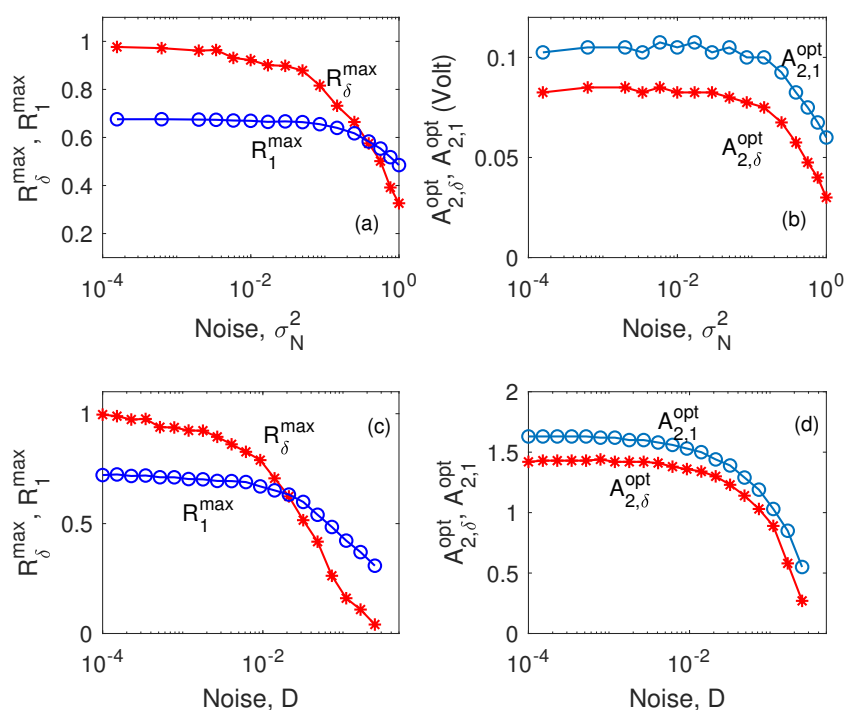


FIG. 5. (a) and (c) Maximal values of the response amplitude at the frequencies δ (R_δ) and f_1 (R_1), (b) and (d) the optimal values of the amplitude of the control signal A_2 depending on the amplitude of the added noise noise intensity. At the top of the plot, the experiment; in the bottom of the plot, the simulation. The control signal at the frequency f_2 .

Acknowledgement

Research project No. F22KI-020.

This work was supported by the Belarusian Republican Foundation for Fundamental

References

- [1] R. Benzi, A. Sutera, and A. Vulpiani, The mechanism of stochastic resonance, *Journ. Phys. A* **14**, L453 (1981).
- [2] P. S. Landa and P. V. E. McClintock, Vibrational resonance, *J. Phys. A: Math. Gen.* **33**, L433 (2000).
- [3] I. I. Blekhman and P. S. Landa, Conjugate resonances and bifurcations in nonlinear systems under biharmonic excitation, *Int. J. Non-Linear Mech.* **39**, 421 (2004).
- [4] V. N. Chizhevsky, Analytical study of vibrational resonance in an overdamped bistable oscillator, *Int. J. Bifurcation and Chaos* **18**, 1767 (2008).
- [5] A. A. Zaikin, L. López, J. P. Baltanás, J. Kurths, and M. A. F. Sanjuán, Vibrational resonance in a noise-induced structure, *Phys. Rev. E* **66**, 011106 (2002).
- [6] J. P. Baltanás, L. López, I. I. Blechman, P. S. Landa, A. Zaikin, J. Kurths, and M. A. F. Sanjuán, Experimental evidence, numerics, and theory of vibrational resonance in bistable systems, *Phys. Rev. E* **67**, 066119 (2003).
- [7] E. Ullner, A. Zaikin, J. García-Ojalvo, R. Bóscos, and J. Kurths, Vibrational

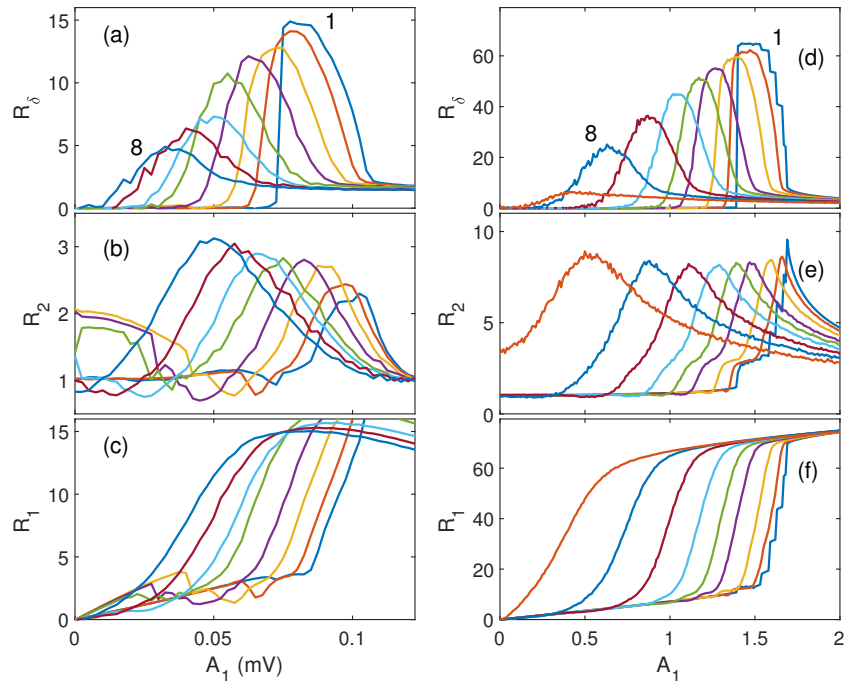


FIG. 6. Response of a VCSEL (the left panel) and overdamped bistable system (the right panel) at the frequencies (a) and (d) δ (R_δ), (b) and (e) f_2 (R_2), (c) and (f) f_1 (R_2) for different values of added noise intensity increasing from '1' to '8' in the plots. Control signal at the frequency f_1 .

resonance and vibrational propagation in excitable systems, *Physics Letters A* **312**, 348 (2003).

- [8] M. Bordet and S. Morfu, Experimental and numerical study of noise effects in a FitzHugh-Nagumo system driven by a biharmonic signal, *Chaos, Solitons and Fractals* **54**, 82 (2013).
- [9] R. Jothimurugan, K. Thamilmaran, S. Rajasekar, and M. A. F. Sanjuán, Experimental evidence for vibrational resonance and enhanced signal transmission in chua's circuit, *Int. J. Bifurcation and Chaos* **23**, 1350189 (2013).
- [10] V. N. Chizhevsky, E. Smeu, and G. Giacomelli, Experimental evidence of "vibrational resonance" in an optical system, *Phys. Rev. Lett.* **91**, 220602 (2003).
- [11] V. N. Chizhevsky and G. Giacomelli, Experimental and theoretical study of the noise-induced gain degradation in vibrational resonance, *Phys. Rev. E* **70**, 062101 (2004).
- [12] V. N. Chizhevsky and G. Giacomelli, Improvement of signal-to-noise ratio in a bistable optical system: Comparison between vibrational and stochastic resonance, *Phys. Rev. A* **71**, 011801(R) (2005).
- [13] V. N. Chizhevsky and G. Giacomelli, Experimental and theoretical study of vibrational resonance in a bistable system with asymmetry, *Phys. Rev. E* **73**, 022103 (2006).
- [14] V. Chizhevsky, Amplification of an autodyne signal in a bistable vertical-cavity surface-emitting laser with the use of a vibrational resonance, *Tech. Phys. Lett.* **44**, 17 (2018).
- [15] V. Chizhevsky, Amplification of optical signals in a bistable vertical-cavity surface-emitting laser by vibrational resonance, *Philos. Trans. Royal Soc. A* **379**, 20200241 (2021).
- [16] A. Wickenbrock, P. C. Holz, N. A. A. Wahab, P. Phoonthong, D. Cubero, and F. Renzoni, Vibrational mechanics in an optical lattice: Controlling transport via potential renormalization, *Phys. Rev. Lett.* **108**, 020603 (2012).
- [17] A. Abusoua and M. F. Daqaq, Experimental Evidence of Vibrational Resonance in a Mechanical Bistable Twin-Well Oscillator, *J Comp Nonlin Dyn* **13** (2018).
- [18] A. Chowdhury, M. G. Clerc, S. Barbay,

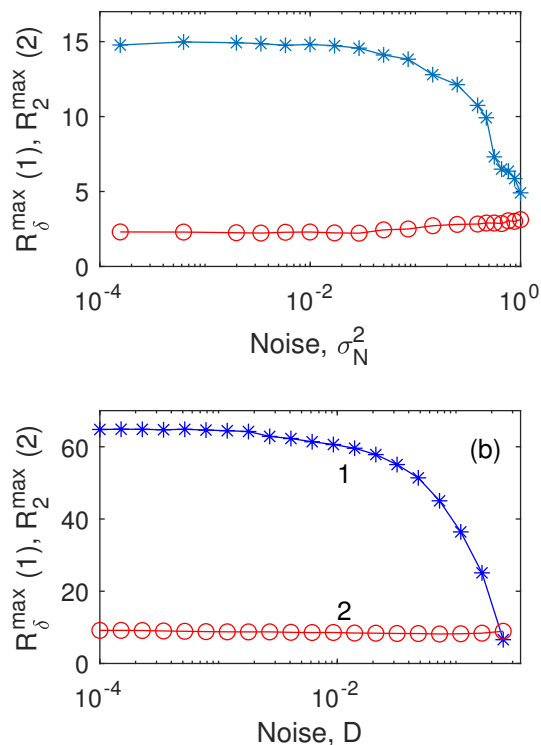


FIG. 7. Maximum values of the response amplitude of the bistable system at frequencies δ and f_2 depending on the amplitude of the added noise D . Control signal at the frequency f_1 . $A_1 = 0.15$, $f_1 = 0.001$, $f_2 = 0.0021$

I. Robert-Philip, and R. Braive, Weak signal enhancement by nonlinear resonance control in a forced nano-electromechanical resonator, *Nature Communications* **11**, 2400 (2020).

- [19] G. Madiot, S. Barbay, and R. Braive, Vibrational resonance amplification in a thermo-optic optomechanical nanocavity, *Nano Letters* **21**, 8311 (2021).
- [20] D. Cubero, J. P. Baltanas, and J. Casado-Pascual, High-frequency effects in the fitzhugh-nagumo neuron model, *Phys. Rev. E* **73**, 061102 (2006).
- [21] B. Deng, J. Wang, and X. Wei, Effect of chemical synapse on vibrational resonance in coupled neurons, *Chaos* **19**, 013117 (2009).
- [22] B. Deng, J. Wang, X. Wei, K. M. Tsang, and W. L. Chan, Vibrational resonance in neuron populations, *Chaos* **20**, 018001 (2010).
- [23] L. Yang, W. Liu, M. Yi, C. Wang, Q. Zhu, X. Zhan, and Y. Jia, Vibrational resonance induced by transition of phase-locking modes in excitable systems, *Phys. Rev. E* **86**, 016209 (2012).
- [24] V. M. Gandhimathi, S. Rajasekar, and J. Kurths, Vibrational and stochastic resonances in two coupled overdamped anharmonic oscillators, *Physics Letters A* **360**, 279 (2006).
- [25] C. Yao and M. Zhan, Signal transmission by vibrational resonance in one-way coupled bistable systems, *Phys. Rev. E* **81**, 061129 (2010).
- [26] J. H. Yang and X. B. Liu, Delay-improved signal propagation in globally coupled bistable systems, *Physica Scripta* **83**, 065008 (2011).
- [27] C.-J. Fang and X.-B. Liu, Theoretical analysis on the vibrational resonance in two coupled overdamped anharmonic oscillators, *Chinese Physics Letters* **29**, 050504 (2012).
- [28] S. Rajasekar, K. Abirami, and M. A. F. Sanjuán, Novel vibrational resonance in multistable systems, *Chaos* **21**, 033106 (2011).
- [29] J. H. Yang and X. B. Liu, Controlling vibrational resonance in a multistable system by time delay, *Chaos* **20**, 033124 (2010).
- [30] J. H. Yang and H. Zhu, Vibrational resonance in duffing systems with fractional-order damping, *Chaos* **22**, 013112 (2012).
- [31] K. P. Harikrishnan and G. Ambika, Resonance phenomena in discrete systems with bichromatic input signal, *European Physical Journal B* **61**, 343 (2008).
- [32] H. Yu, J. Wang, C. Liu, B. Deng, and X. Wei, Vibrational resonance in excitable neuronal systems, *Chaos* **21**, 043101 (2011).
- [33] S. Rajasekar, J. Used, A. Wagemakers, and M. A. F. Sanjuán, Vibrational resonance in biological nonlinear maps, *Commun. Nonlin. Sci. Numer. Simul.* **17**, 3435 (2012).
- [34] S. Rajasekar and M. A. F. Sanjuán, *Nonlinear Resonances* (Springer Series in Synergetics, 2016).
- [35] T. O. Roy-Layinde, U. E. Vincent, S. A. Abolade, O. O. Popoola, J. A. Laoye, and P. V. E. McClintock, Vibrational resonances in driven oscillators with position-dependent mass, *Philos. Trans. Royal Soc. A* **379**, 20200227 (2021).
- [36] U. E. Vincent, P. V. E. McClintock, I. A. Khovanov, and S. Rajasekar, Vibrational and stochastic resonances in driven nonlinear systems: part 2, *Philos. Trans. Royal Soc. A* **379**, 20210003 (2021).
- [37] C. Yao, Y. Liu, and M. Zhan, Frequency-resonance-enhanced vibrational resonance in bistable systems, *Phys. Rev. E* **83**, 061122

- (2011).
- [38] S. Rajamani, S. Rajasekar, and M. A. F. Sanjuán, Ghost-vibrational resonance, *Commun. Nonlin. Sci. Numer. Simul.* **19**, 4003 (2014).
- [39] K. Abirami, S. Rajasekar, and M. A. F. Sanjuán, Vibrational and ghost-vibrational resonances in a modified chua's circuit model equation, *Int. J. Bifurcation Chaos* **24**, 1430031 (2014).
- [40] B. Usama, S. Morfu, and P. Marquie, Vibrational resonance and ghost-vibrational resonance occurrence in chuas circuit models with specific nonlinearities, *Chaos, Solitons and Fractals* **153**, 111515 (2021).
- [41] V. N. Chizhevsky, Vibrational higher-order resonances in an overdamped bistable system with biharmonic excitation, *Phys. Rev. E* **90**, 042924 (2014).
- [42] J. H. Yang, M. A. F. Sanjuán, and H. G. Liu, Vibrational subharmonic and superharmonic resonances, *Commun. Nonlin. Sci. Numer. Simul.* **30**, 362 (2016).
- [43] J. Casado-Pascual and J. P. Baltanas, Effects of additive noise on vibrational resonance in a bistable system, *Phys. Rev. E* **69**, 046108 (2004).
- [44] F. Guo and X.-F. Cheng, Vibrational resonance in a bistable system with multiplicative and additive noise, *Journal of the Korean Physical Society* **58**, 1567 (2011).
- [45] S. Jeyakumari, V. Chinnathambi, S. Rajasekar, and M. A. F. Sanjuán, Vibrational resonance in an asymmetric duffing oscillator, *Int. J. Bifurcation and Chaos* **21**, 275 (2011).
- [46] Y. Qin, J. Wang, C. Men, B. Deng, and X. Wei, Vibrational resonance in feedforward network, *Chaos* **21**, 023133 (2011).
- [47] J. Casado-Pascual, D. Cubero, and J. P. Baltanas, Stochastic resonance with weak monochromatic driving: Gains above unity induced by high-frequency signals, *EPL* **77**, 50004 (2007).
- [48] V. N. Chizhevsky, Noise-induced suppression of nonlinear distortions in a bistable system with biharmonic excitation in vibrational resonance, *Phys. Rev. E* **92**, 032902 (2015)